JOURNAL OF SOLID STATE CHEMISTRY 54, 54–60 (1984)

New Ferromagnetic Materials for Magnetic Recording: The Iron Carbonitrides

D. ANDRIAMANDROSO, G. DEMAZEAU, M. POUCHARD, AND P. HAGENMULLER

Laboratoire de Chimie du Solide du CNRS, 351 cours de la Libération, 33405 Talence Cedex, France

Received January 11, 1984

New ferromagnetic materials derived from iron nitride Fe_4N by partial substitution of nitrogen by carbon have been prepared by nitriding the iron oxalate whose thermal decomposition gives a carburating atmosphere. The morphology of the carbonitride crystallites depends on the elaboration conditions of the precursor. The particle shapes have been examined by electron microscopy. The coercive field can be improved by partially replacing iron by tin. For a composition close to $Fe_3Fe_{0.6}Sn_{0.4}N_{0.7}C_{0.3}$ the coercive field reaches 600 Oe. The average size of the microcrystallites was determined by X-ray diffractometry. An investigation of the aging of the material has been also carried out.

I. Introduction

The development of magnetic recording techniques is largely related to that of magnetic particles suitable for sensitive coatings on tapes or disks. The magnetic requirements that such materials must satisfy are the high coercive field H_c and saturation magnetization σ_s, and large remanence ratio σ_r/σ_s. Thermal stability in the temperature range concerned, and morphological properties related to the recording process are also required.

For a given material, the coercive field can be improved in the following three ways:

—by reducing the particle size down to the critical size of magnetic single domains,

—by enhancing the shape anisotropy (acicular particles) if allowed by the recording procedure,

—by increasing the magnetocrystalline anisotropy in the bulk or at the surface.

The magnetic materials that have been developed during the last 20 years are essentially γ-Fe_2O_3, CrO_2, and metallic particles.

In the spinel γ-Fe_2O_3 ($\sigma_{0s} \simeq 84$ emu $\cdot$ g^{-1}), the magnetocrystalline anisotropy can be increased by using doping agents like Co(II) (ground term $^4T_{1g}$), either by substitution in the lattice (*1, 2*) or by diffusion on the surface (*3, 4*). For the rutile-type CrO_2 ($\sigma_{0s} \simeq 92$ emu $\cdot$ g^{-1}) the coercive field has been improved by increasing the particle-shape anisotropy: seeds incorporated in the CrO_3 reduction process impose the orientation of the acicular growth (*5–7*). In contrast, in the Cr_2O_3 oxidation process (*8*), even higher coercive fields have been obtained (*9, 10*) by increasing the magnetocrystalline anisotropy of the CrO_2 particles

0022-4596/84 $3.00

by partial substitution of Cr(IV) either by Rh(IV) or by Ir(IV) ($^2T_{2g}$). Ferromagnetic metallic particles (e.g., iron or iron alloys) have also been used, but the high magnetic properties ($H_c \simeq 1000$ Oe, $\sigma_{0s} \simeq 218$ emu · g^{-1}) (*11*), are offset by easy atmospheric oxidation of the metal even under normal working conditions, which requires complete environmental protection. To achieve a significant improvement, any new recording material must have magnetic properties comparable to those of iron particles and simultaneously a better stability against an oxidation.

Iron nitrides, in particular Fe_4N, in which iron is stabilized by the presence of nitrogen, satisfy some of the previous requirements fairly well: σ_{0s} (Fe_4N) $\simeq$ 208 emu · g^{-1}. They have been subject to several fundamental studies dealing with crystal and magnetic structures (*12–15*). Their possibilities for magnetic recording have been investigated, particularly in Japan (*16, 17*).

Although Fe_4N is more stable to the action of oxygen than the metallic particles, in the finely divided form used in tapes, it will still oxidize. However, insertion of carbon into the lattice might increase its stability in air. We have therefore investigated the possibility of preparing such carbonitrides for use in magnetic recording.

At low temperature (θ = 400°C) and under nitriding conditions (NH_3/H_2 gas flow), all Fe compounds, which give off CO during thermal decomposition undergo simultaneously carburization ($2CO \rightleftarrows C + CO_2$). Ferrous oxalate, which has been chosen as a precursor, crystallizes mostly as needles and was therefore thought to yield pseudomorphs, which might lead to acicular carbonitrides.

II. Preparation and Morphological and Magnetic Characteristics of the Particles

Two types of equipments were used: a fluidized bed reactor and a conventional furnace. In each case formation of the carbonitride required simultaneous thermal decomposition of the oxalate precursor and nitridation.

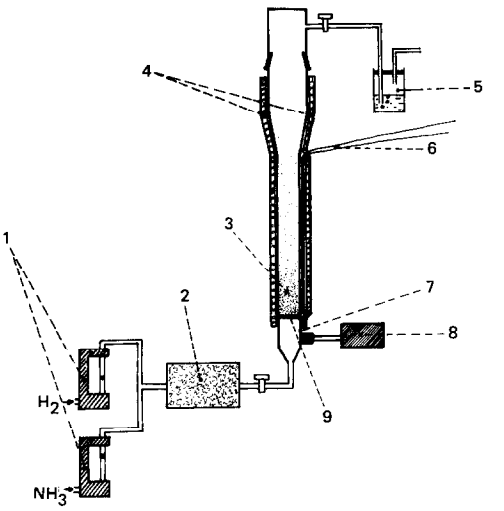

FIG. 1. Schematic diagram of a fluidized bed reactor. (1) Gas flow gauge. (2) Preheating device for gas flow. (3) Material. (4) Heating ribbon. (5) Bubble bath. (6) Thermocouple. (7) Quartz tube. (8) Vibrator. (9) Porous glass.

(*a*) *Preparation in Conventional Furnace*

A certain amount of the precursor was spread out uniformly in an alumina boat put in a quartz tube. A mixture of NH_3 and H_2 with a ratio close to 1/3.2 crossed the tube at 400°C for about 6 hr. When the reaction was completed, the gas flow was stopped and the tube was flushed with N_2 for 5 min in order to drive out the residual gas and then cooled down to room temperature. The resulting material was immersed directly into cold toluene to prevent eventual combustion in air. It was then washed and dried. The X-ray powder pattern characterized a single phase similar to the cubic Fe_4N phase.

(*b*) *Preparation in Fluidized Bed Reactor*

Figure 1 shows schematically the generating set. The precursor was placed in the quartz tube. The temperature was raised up

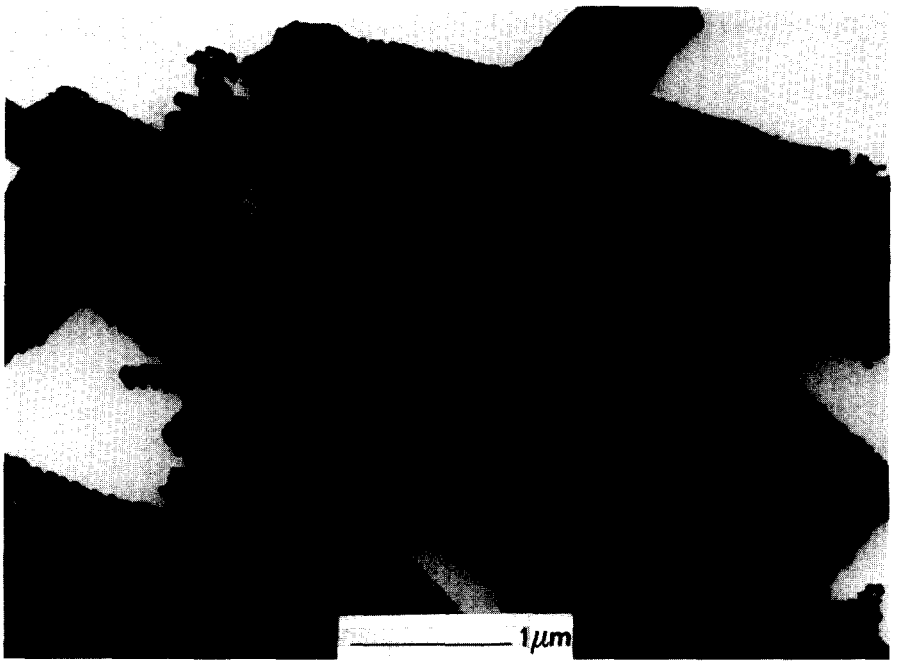

FIG. 2. Electron transmission micrography of $Fe_4N_{1-\varepsilon}C_\varepsilon$.

to 400°C by means of a heating ribbon wrapped along the tube and a preheated NH_3/H_2 gas mixture (NH_3/H_2 ratio close to 1.4) was passed through the reaction cell.

The reaction time varied from 3 to 5 hr. At the end of the reaction, the tube was cooled down to room temperature and the NH_3/H_2 flow replaced by nitrogen. The sample was plunged into cold toluene, washed, and dried. The X-ray powder pattern of the product revealed again a single phase similar to Fe_4N.

Depending on the apparatus used and the temperature and duration of the reaction, the coercive field varied from 300 to 500 Oe. The saturation magnetization at 25°C was of the order of 120 emu · g^{-1}.

TEM showed acicular particles retaining the shape of the oxalate crystals (pseudomorphism) (Fig. 2), but each particle was an aggregate of small crystallites. A conventional carbon analysis carried out on some of the products obtained from a conventional furnace gave a carbon rate from 5.8 to 6% (at.%). It leads approximately to the formulation $Fe_4N_{0.7}C_{0.3}$. The analysis by Auger spectroscopy of such particles gave an average percentage of nitrogen (14%) in agreement with the proposed formulation. In addition the same analysis leads to carbon contents close to 7% at the surface of the particles and 4% after stripping the surface of about 800 Å. This result shows that carbon is localized preferentially on the crystal surface.

III. Improvement of the Morphological Characteristics

To increase the coercive field of the material the elementary crystallites constituting the particles must be small enough to be magnetic single domains. Two routes were possible to achieve these results:

(i) A control of the size and the morphology of the precursor crystallites during the

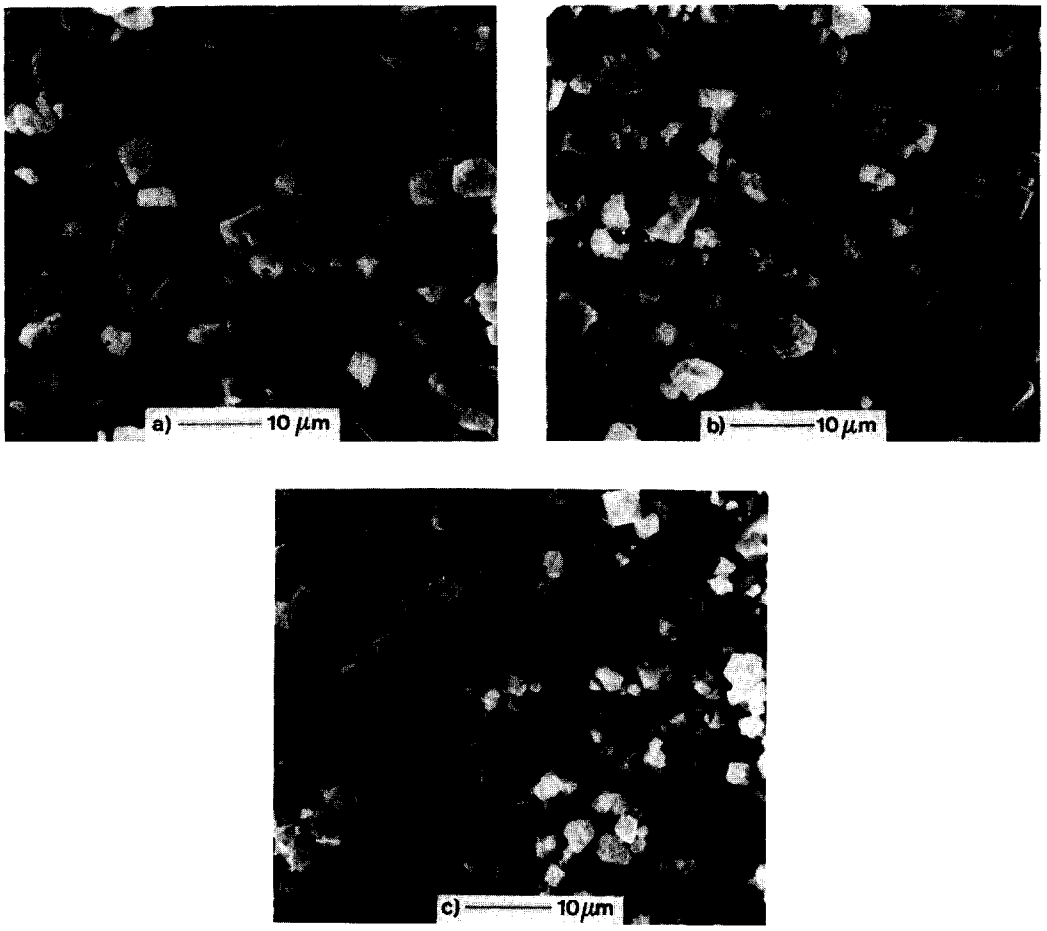

FIG. 3. Scanning electron micrograph of iron oxalate prepared from oxalic acid (pH 2) and a ferrous salt solution with (a) = $Fe^{2+} = 5 \times 10^{-3}$ *M*, (b) = $Fe^{2+} = 5 \times 10^{-2}$ *M*, (c) = $Fe^{2+} = 10^{-1}$ *M*.

oxalate elaboration, either by checking the pH or the iron concentration or by the use of crystal growth initiators.

(ii) A reduction of the size of the elementary crystallites using dopants as limiting crystal growth initiators.

III-1. Controlling the Size and the Morphology of the Carbonitride Particles at the Precursor Stage

III-1-1. Optimal experimental conditions for the precipitation of the oxalate precursor. The control of the oxalate precipitation conditions (pH, iron salt concentration) allows size and shape of the precursor's crystallites to be modified. In a solution of oxalic acid at constant pH, the average size of the oxalate particles decreased when the concentration of the reacting ferrous salt (chloride or sulfate) increased. At the same time the acicularity (*L*/*l*) decreased from 3 to 1.5 (Fig. 3).

At a constant concentration of ferrous salt and with increasing pH of the oxalic acid, the average size of the particles decreased again, but the corresponding acicularity of the oxalate crystals increased from 2.5 to about 4. The combination of those

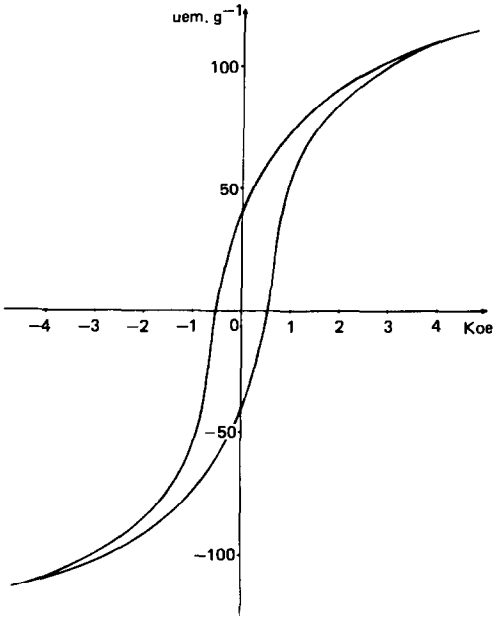

FIG. 4. Hysteresis loop of $Fe_4N_{1-\varepsilon}C_\varepsilon$ (σ_s (10 Koe) = 120 emu · g^{-1}, H_c = 530 Oe).

different experimental factors governing the oxalate preparation can be used to modify the size and the desired morphology of the precursor and in turn, thanks to pseudomorphism, those of the deriving carbonitride.

III-1-2. Decrease of the precursor particle size using crystal growth initiator. To obtain small-size particles of greater acicularity, we used rare-earth (in particular La and Nd) oxalates as growth initiators. Lanthanum oxalate could be precipitated before iron oxalate by adding a small amount of a lanthanum salt (La/(La + Fe) < 0.05) to the solution of the ferrous salt (the solubility products under normal conditions are 2×10^{-28} for lanthanum oxalate and 2×10^{-7} for iron oxalate). The particles of the La oxalate play the role of crystallization nuclei for Fe oxalate. Thus after carbonitridation, samples were obtained with a coercive field reaching 530 Oe (Fig. 4).

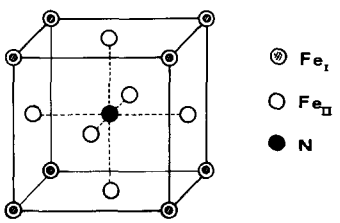

FIG. 5. Structure of iron nitride (Fe_4N).

III-2. Control of the Morphology and Size of the Elementary Crystallites of Carbonitrides Using Tin as a Limiting Crystal Growth Agent

Tin which substitutes for iron in Fe_4N preferentially at site I (*18*) (Fig. 5), is able to modify the crystal growth of the elementary particles of the carbonitrides. We have therefore studied the system $Fe_3^{II}Fe_{1-x}^{I}Sn_xN_{1-\varepsilon}C_\varepsilon$.

The preparation conditions were similar for all samples: $\theta \simeq 400°C$, $t \simeq 6$ h, $NH_3/H_2 \simeq 0.3$). The resulting ε value was practically constant, about 0.3 (i.e., corresponding to ca. 6 at.% C). The materials has been prepared from coprecipitated Fe and Sn oxalates. The Sn content was determined with a flame spectrophotometer.

The variation of the coercive field with x is given in Fig. 6. The coercive field for $x \simeq 0.4$ was close to 600 Oe.

TEM revealed that the size of the elementary microcrystallites decreased with increasing x. The average size of the microcrystallites was determined by X-ray diffraction from the relation

$$L_c = K\lambda/\beta \cos \theta,$$

where K is the Scherrer constant ($\simeq 0.9$) and β the half-width of the X-ray line in radians. In agreement with electron microscopy L_c was found to decrease with increasing x (*19*) (Fig. 7). In addition those results were confirmed by Mössbauer spectroscopy: the number of superparamagnetic particles increased with x (*20*).

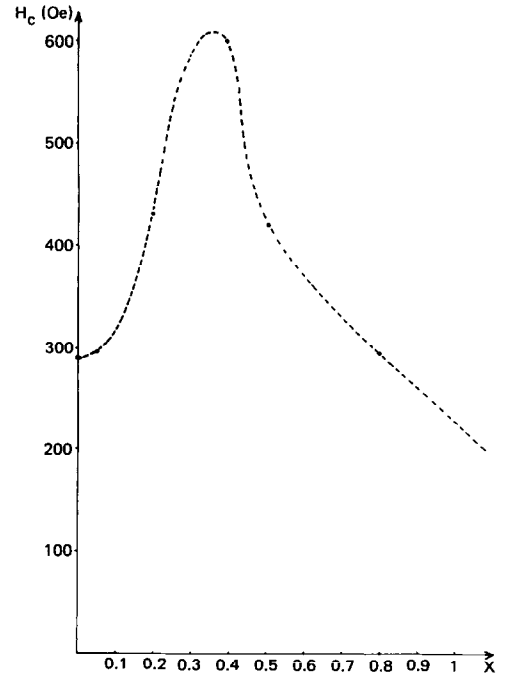

FIG. 6. Variation of coercive field of $Fe_3Fe_{1-x}Sn_xN_{1-\varepsilon}C_\varepsilon$ with x.

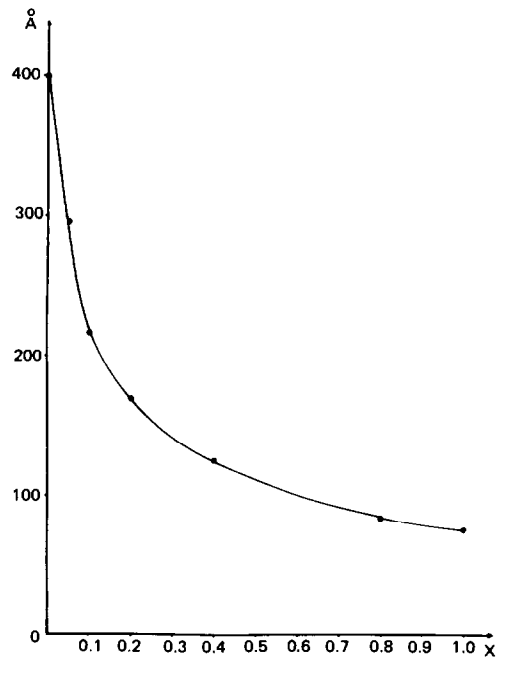

FIG. 7. Variation in the average size of microcrystallites of $Fe_3Fe_{1-x}Sn_xN_{1-\varepsilon}C_\varepsilon$ with x ($\varepsilon \simeq 0.3$).

TABLE I

	A	B
$\sigma_s(f)/\sigma_s(i)$	0.83	0.90
$\sigma_4(f)/\sigma_r(i)$	0.896	0.91
Final X-ray analysis	Fe_4N + $Fe_\alpha(N)$ + iron oxide	Fe_4N + $Fe_\alpha(N)$

Note. A = conventional Fe_4N, B = iron carbonitride $Fe_4N_{1-\varepsilon}C_\varepsilon$, f = final, i = initial.

IV. Comparison of the Stability in Air of Carbonitrides and Conventional Fe_4N

A comparative study was carried out on the stability in air of Fe_4N prepared in conventional manner and isostructural carbonitride obtained by the previous methods. The materials were submitted to a severe aging test (100% hygroscopicity, $\theta \simeq 70°C$) for 10 weeks. The result is shown in Table I. We found that the $\sigma_{fin.}/\sigma_{in.}$ ratios decreased more slowly for the carbonitride than for conventional Fe_4N. Also the appearance of small lines corresponding to Fe_3O_4 in the X-ray spectrum of the conventional Fe_4N product suggests that the carbonitride is more stable in air.

V. Conclusions

The size and shape of the carbonitride particles can be controlled by modifying the conditions of preparation of the oxalate precursor. Small oxalate particles are obtained by using rare-earth oxalates as crystal growth initiators.

Auger spectroscopy indicates that carbon atoms substitute preferentially at surface sites of the particles.

An investigation of the $Fe_3Fe_{1-x}Sn_xN_{1-\varepsilon}C_\varepsilon$ solid solutions has shown that Sn plays the role of a growth inhibitor of the elementary microcrystallites of the carbonitride. Doping with tin can thus raise the value of H_c. For $x \simeq 0.4$ the coercive field attains 600 Oe.

An aging test in air suggests that the magnetic properties of the iron carbonitrides derived from Fe_4N changed less with time and temperature than those of Fe_4N prepared by a conventional method.

Such a stability in air, the high magnetic performances (close to those of metallic particles), and the flexibility in the modification of the particle morphology allow to consider the iron carbonitrides as a new promising set of materials for magnetic recording.

References

1. P. Mollard, A. Collomb, J. Devenyi, A. Rousset, and J. Paris, *IEEE Trans. Magn. MAG 11* **3,** 894 (1975).
2. E. Köster, *IEEE Trans. Magn. MAG 8* **3,** 428 (1972).
3. Y. Imaoka, S. Umeki, Y. Kubota, and Y. Tokuoka, *IEEE Trans. Magn. MAG 14* **5,** 649 (1978).
4. Y. Kubota, H. Morita, Y. Tokuoka, and Y. Imaoka, *IEEE Trans. Magn. MAG 15* **6,** 1558 (1979).
5. K. E. Naumann and E. D. Daniel, *J. Audio Eng. Soc.* **19,** 822 (1971).
6. L. K. Jordan, R. J. Kerr, and J. E. Dickens, *J. Audio Eng. Soc.* **20,** 2 (1972).
7. D. M. Miller, *J. Appl. Phys.* **49,** 1821 (1978).
8. G. Demazeau, P. Maestro, T. Plante, M. Pouchard, and P. Hagenmuller, *Ann. Chim. Sci. Matér.* **3,** 353 (1978).
9. G. Demazeau, P. Maestro, T. Plante, M. Pouchard, and P. Hagenmuller, *Mater. Res. Bull.* **14,** 121 (1979).
10. P. Maestro, D. Andriamandroso, G. Demazeau, M. Pouchard, and P. Hagenmuller, *IEEE Trans. Magn. MAG 18* **5,** 1000 (1982).
11. G. Bate, *J. Appl. Phys.* **52**(3), 2447 (1981).
12. K. H. Jack, *Proc. R. Soc. A* **195,** 34 (1948).
13. G. W. Wiener and J. A. Berger, *J. Met.* **7,** 360 (1955).
14. B. C. Frazer, *Phys. Rev.* **112,** 751 (1958).
15. S. Nagakura, *J. Phys. Soc.* **25**(2), 488 (1968).
16. S. Suzuki, H. Sakumoto, J. Minegishi, and Y. Omote, *IEEE Trans. Magn. MAG 17* (**6**), 3017 (1981).
17. K. Tagawa, E. Kita, and A. Tasaki, *J. Phys. Soc.* **21**(11), 1596 (1982).
18. G. Shirane, W. J. Takei, and S. L. Ruby, *Phys. Rev.* **126,** 49 (1962).
19. F. W. Jones, *Proc. R. Soc. A* **166,** 16 (1938).
20. D. Andriamandroso, L. Fefilatiev, G. Demazeau, L. Fournes, M. Pouchard, and P. Hagenmuller, *Mater. Res. Bull.*, in press.